Title 論文題目	Involvement of necroptosis in contrast-induced nephropathy in a rat CKD model （ラット慢性腎臓病モデルにおける造影剤腎症へのネクロプトーシスの関与）
Author(s) 著者	柴田, 智
Degree number 学位記番号	乙第3143号
Degree name 学位の種別	博士(医学)
Issue Date 学位取得年月日	2021-09-21
Original Article 原著論文	Clin Exp Nephrol. 2021 Jul;25(7):708-717
Doc URL	
DOI	10.1007/s10157-021-02048-1
Resource Version	Author Edition

Clinical and Experimental Nephrology (2021) 25:708–717
https://doi.org/10.1007/s10157-021-02048-1

ORIGINAL ARTICLE

Involvement of necroptosis in contrast-induced nephropathy in a rat CKD model

Satoru Shibata[1] · Norihito Moniwa[1] · Atsushi Kuno[1] · Ayumu Kimura[1] · Wataru Ohwada[1] · Hirohito Sugawara[1] · Yufu Gocho[1] · Marenao Tanaka[1] · Toshiyuki Yano[1] · Masato Furuhashi[1] · Masaya Tanno[1] · Takayuki Miki[1] · Tetsuji Miura[1]

Received: 6 August 2020 / Accepted: 8 March 2021 / Published online: 16 March 2021

Abstract

Background The risk of contrast-induced nephropathy (CIN) is high in patients with chronic kidney disease (CKD). However, the mechanism of CIN in CKD is not fully understood. Here, we prepared a clinically relevant model of CIN and examined the role of necroptosis, which potentially cross-talks with autophagy, in CIN.

Methods In Sprague–Dawley rats, CKD was induced by subtotal nephrectomy (SNx, 5/6 nephrectomy) 4 weeks before induction of CIN. CIN was induced by administration of a contrast medium (CM), iohexol, following administration of indomethacin and *N*-omega-Nitro-L-arginine methyl ester. Renal function and tissue injuries were assessed 48 h after CM injection.

Results Serum creatinine (s-Cre) and BUN were increased from 0.28 ± 0.01 to 0.52 ± 0.02 mg/dl and from 15.1 ± 0.7 to 29.2 ± 1.2 mg/dl, respectively, after SNx alone. CM further increased s-Cre and BUN to 0.69 ± 0.03 and 37.2 ± 2.1, respectively. In the renal tissue after CM injection, protein levels of receptor-interacting serine/threonine-protein kinase (RIP) 1, RIP3, cleaved caspase 3, and caspase 8 were increased by 64 ~ 212%, while there was reduction in LC3-II and accumulation of p62. Necrostatin-1, an RIP1 inhibitor, administered before and 24 h after CM injection significantly suppressed elevation of s-Cre, BUN and urinary albumin levels, kidney injury molecule-1 expression and infiltration of CD68-positive macrophages in renal tissues after CM injection.

Conclusion The results suggest that necroptosis of proximal tubular cells contributes to CIN in CKD and that suppression of protective autophagy by pro-necroptotic signaling may also be involved.

Keywords Contrast-induced nephropathy · Necroptosis · RIP1 · Subtotal nephrectomy

Introduction

Contrast-induced nephropathy (CIN) is a major cause of acute renal failure during hospitalization and many cases of CIN occur in patients undergoing cardiac catheterization and percutaneous coronary intervention [1]. There are multiple risk factors for CIN. Azzalini et al. [2] categorized the risk factors into patient-related factors including pre-existing chronic kidney disease (CKD) and procedure-related factors including the use of a large volume of contrast medium (CM) and high-osmolar CM [2]. Mehran et al. [3] reported that the incidence of CIN in patients with no risk factors was ~ 5% and that the combination of risk factors elevated the risk of CIN to 50 ~ %. CIN is associated with increases in mortality and cardiovascular events [1]. However, preventive measures or therapy for CIN have not been established.

The mechanisms of CIN include intra-renal hemodynamic changes and direct toxic effects of CMs [4–6]. CMs induce vasoconstriction and hypoxia in the medullary region, leading to reduction of glomerular blood flow and tubular cell ischemia [4]. Detrimental effects of CMs on renal tubular cells include activation of proinflammatory and proapoptotic signaling pathways and impairment

Satoru Shibata and Norihito Moniwa equally contributed to this work.

✉ Norihito Moniwa
moniwa@sapmed.ac.jp

[1] Department of Cardiovascular, Renal and Metabolic Medicine, Sapporo Medical University School of Medicine, S-1, W-16, Chuo-ku, Sapporo 060-8543, Japan

of protective autophagy [7]. Recently, roles of necroptosis, a novel form of programmed cell death, in renal diseases such as ischemia/reperfusion injury [8] and CKD [9] have received attention. However, the contribution of necroptosis to CIN has not been clarified.

In the present study, we aimed to clarify the contribution of necroptosis to CIN in a clinically relevant animal model. Since CKD is a major risk factor of CIN [1–3, 10], we prepared a model of CIN in pre-existing CKD. In addition to pro-necroptosis signaling, autophagy-regulating signal in CIN was examined, since we recently found important cross-talk between necroptosis and autophagy in cardiomyocytes [11, 12].

Materials and methods

This study was approved by the Animal Use Committee of Sapporo Medical University (#16-088) and was conducted in strict accordance with the Guide for the Care and Use of Laboratory Animals published by the United States National Institutes of Health. All animal experiments were performed in the Animal Research Center of Sapporo Medical University.

Animals

Male Sprague–Dawley (SD) rats (Charles River Laboratories, Yokohama, Japan) were housed in a temperature-, humidity-, and light-controlled room and given free access to food and water.

Preparation of a 5/6 nephrectomy model of CKD

Rats at ages of 8 weeks were anesthetized with isoflurane (1–2%), and two-stage subtotal nephrectomy (SNx) was performed as previously described [13]. Briefly, the left kidney was removed after ligation of the left renal blood vessels and the left ureter. Seven days later, the upper and lower poles of the right kidney were resected.

Induction of CIN

Four weeks after the second surgery, the right common carotid artery and jugular vein were cannulated with a polyethylene tube (PE50) under anesthesia with isoflurane. Twenty-four hours later, each rat was placed in a foam plastic jacket that allowed movement of all four limbs and forward vision. As shown in Fig. 1, isotonic saline was infused intravenously at a rate of 1 ml/kg/h for 4 h to avoid plasma volume depletion. At 2 h after the commencement of saline infusion, CIN was induced according to a protocol previously reported [14]. Briefly, indomethacin (10 mg/kg) and then *N*-omega-Nitro-L-arginine methyl ester (L-NAME, 10 mg/kg) were administered intravenously with a 15-min interval, and then a CM, iohexol (Dai-ichi Sankyo, Japan), at a dose of 1,600 mg I/kg was injected intravenously. After 4-h infusion of saline, rats were returned to individual cages for recovery. After 24 h, rats were placed in metabolic cages for another 24 h for urine collection.

Experimental protocols

Experiments were conducted according to two protocols shown in Fig. 1.

Protocol 1: Assessment of necroptosis and autophagy in CKD and CIN models

Rats were divided into three groups, a Sham group, an SNx group and an SNx + CM group. SNx alone and both SNx and induction of CIN were performed in the SNx group and the SNx + CM group, respectively. Forty-eight hours after administration of indomethacin/L-NAME/

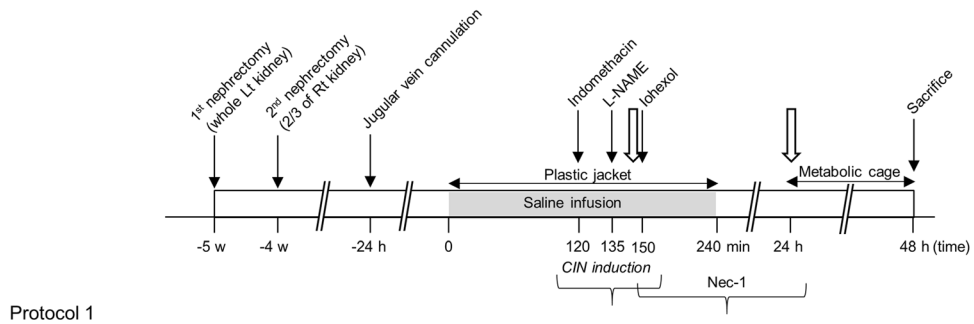

Protocol 1						
Sham	-	-	+	-		
SNx	+	+	+	-		
SNx+CM	+	+	+	+		
Protocol 2						
SNx+CM+Ve	+	+	+	+	-	
SNx+CM+Nec-1	+	+	+	+	+	

Fig. 1 Experimental protocols. Sequences of surgeries, drug administration and tissue sampling in each protocol are shown. In Protocol 1 and Protocol 2, saline was infused at 1 ml/kg/h. *SNx* subtotal nephrectomy, *Sham*: sham operation, *CIN induction* contrast-induced nephropathy induction by indomethacin, L-NAME and iohexol, *Nec-1* necrostatin-1. Open arrows indicate time points of injection of Nec-1 or its vehicle. Minus in the figure stands for sham operation or vehicle administration

iohexol or vehicles, rats were euthanized by deep anesthesia. Kidneys were excised and divided into halves. One half of the tissue was frozen for storage at − 80 °C until analysis, and the other half was fixed in 10% formaldehyde for histological examination.

Protocol 2: Effects of pharmacological inhibition of necroptosis on CIN

Rats that received SNx and induction of CIN were divided into two groups. Necrostatin-1 (Nec-1, 1.65 mg/kg), a necroptosis inhibitor, was intraperitoneally injected immediately before and 24 h after induction of CIN in the SNx + CM + Nec-1 group, while a vehicle was injected at the same time points in the SNx + CM + Ve group. Normal SD rats ($n = 3$) were used as control to evaluate electron micrographs of proximal tubular cells.

Western blotting

Western blotting was performed as previously reported [15] using primary antibodies listed in Table 1. Details are described in Supplementary file1.

Real-time PCR

mRNA levels of KIM-1, IL-1β, TNF-α and MCP-1 in kidneys were determined by real-time PCR as described previously [16]. Details are described in Supplementary file1.

Histological analysis

Renal tubular injury was assessed histologically with Periodic acid-Schiff (PAS) staining and immunostaining for kidney injury molecule-1 (KIM-1) and CD68. Ten images of corticomedullary areas were randomly selected in each kidney sample under magnification of × 200 in light microscopy. The extent of renal tubular injury in PAS-stained sections was quantified by the use of acute tubular necrosis (ATN) score [15] with modifications. ATN score was given according to the percentage of damaged areas in tubules: 0, no damage; 1, < 10%; 2, 11–25%; 3, 26–50%; 4, 51–75%; and 5, > 75%. Tubule damage was classified into cell lysis, tubular dilation, loss of tubular brush border or cast formation. KIM-1 and CD68 staining in renal tissues was performed using an anti-KIM-1 antibody (AF3689, R&D Systems, 1:20) and an anti-CD68 antibody (MCA341R, BIO-RAD, 1:100), respectively. The KIM-1- and CD68-positive areas were determined in ten randomly selected fields from six kidneys in each group under magnification of 100× in light microscopy. The glomerular area was excluded for analyses of KIM-1 and CD68.

Electron microscopy

Renal tissue samples were immersion fixed with 2.5% glutaraldehyde phosphate buffer (pH 7.4) overnight at 4 °C, followed by post fixation with 1% OsO_4. After dehydration, tissues were embedded in epoxy resin. Ultrathin sections at 50 nm were prepared with an ultramicrotome and stained with uranyl acetate and lead citrate for electron microscopy (Hitachi EM 7100 electron microscope, Hitachi High

Table 1 Antibodies used for Western blotting in this study

Antibodies	Source	Cat. No
Rabbit monoclonal anti-LC3A/B (D3U4C) XP	Cell signaling technology	#12741
Guinea pig polyclonal anti-p62/SQSTM1 (C-terminus)	PROGEN	GP62-C
Rabbit monoclonal anti-phospho-AMPKα (Thr172)	Cell signaling technology	#2535
Rabbit polyclonal anti-AMPKα	Cell signaling technology	#2532
Rabbit polyclonal anti-phospho-p70S6 Kinase (Thr389)	Cell signaling technology	#9205
Rabbit polyclonal anti-p70S6 Kinase	Cell signaling technology	#9202
Rabbit polyclonal anti-phospho-S6 Ribosomal Protein (Ser235/236)	Cell signaling technology	#2211
Rabbit monoclonal anti-S6 Ribosomal Protein (5G10)	Cell signaling technology	#2217
Rabbit polyclonal anti-phospho-Akt (Ser473)	Cell signaling technology	#9275
Rabbit polyclonal anti-Akt	Cell signaling technology	#9272
Rabbit polyclonal anti-Bcl-2	Cell signaling technology	#2876
Rabbit monoclonal anti-Beclin-1 (D40C5)	Cell signaling technology	#3459
Mouse monoclonal anti-RIP-1	BD biosciences	610459
Rabbit monoclonal anti-RIP-3	Cell signaling technology	#15828
Rabbit polyclonal anti-Caspase-3	Cell signaling technology	#9662
Rabbit monoclonal anti-Caspase-8 (D35G2)	Cell signaling technology	#4790
Mouse monoclonal anti-vinculin	Sigma-Aldrich	V9131

Technologies Corp., Tokyo, Japan). The extent of ultrastructural damage in tubular cells was quantified by a score system in which one point each was assigned to loss of microvilli, bleb-like protrusion of the apical cytoplasm, increase in vacuoles, swelling and/or displacement of mitochondria, displacement of the nucleus, and disruption of the plasma membrane in a cross-section of each proximal tubule. Six electron microscopy images under magnification of 2000× were randomly selected in each kidney sample ($n=3$ in each treatment group) for calculation of total score of the ultrastructural damage, in which 106 ~ 124 tubular cells per treatment group were examined.

Statistical analysis

All values are presented as means ± SEM. One-way ANOVA followed by Tukey's post hoc test was used for testing differences between three groups except ultrastructural tubular damage score. Kruskal–Wallis test followed by the Dunn's test was used to compare ultrastructural tubular damage scores between three groups. Differences in group mean data except ATN score between two groups were tested by unpaired Student's *t* test. Mann–Whitney *U* test was used to compare ATN scores between groups. Data for urine albumin-to-creatinine ratio (uACR) were normalized by logarithmic transformation, because uACR showed a non-normal distribution ($p<0.05$ in both protocols) and log uACR showed a normal distribution ($p=0.59$ in Protocol 1 and $p=0.91$ in Protocol 2) by the Shapiro–Wilk test (Figs. S1 and S2). Statistical analyses were performed using GraphPad PRISM Version 8.1.2 (GraphPad, San Diego, CA) and differences were considered significant when the *p* value was less than 0.05.

Results

Profile of renal dysfunction in CKD and CIN models

Data for blood pressure, renal function and weights of the heart and kidneys in Protocol 1 are summarized in Table 2. Levels of s-Cre, BUN and log uACR and heart weight-to-body weight ratio were significantly higher in the SNx group than in the Sham group, confirming a phenotype of CKD in the SNx group. There were trends for reduced body weight and for elevation of blood pressure in the SNx group. Levels of s-Cre and BUN were higher in the SNx + CM group than in the SNx group, indicating development of CIN. Log uACR was also larger in the SNx + CM group than in the SNx group, but the difference was not statistically significant. Kidney weight-to-body weight ratio was larger in the SNx + CM group than in the SNx group, suggesting renal edema after CM injection.

Table 2 Blood pressure and renal function data in Protocol 1

	Sham	SNx	SNx + CM
N	6	17	16
BW (g)	444.2 ± 10.9	412.9 ± 8.2	409.4 ± 7.7
SBP (mmHg)	113.3 ± 1.3	125.1 ± 6.0	129.1 ± 4.1
DBP (mmHg)	77.7 ± 3.5	86.4 ± 4.5	91.6 ± 2.4
s-Cre (mg/dl)	0.28 ± 0.01	0.52 ± 0.02*	0.69 ± 0.03*,†
BUN (mg/dl)	15.1 ± 0.7	29.2 ± 1.2*	37.2 ± 2.1*,†
Log uACR (mg/gCre)	3.43 ± 0.63	5.08 ± 1.75*	5.92 ± 0.24*
Na (mEq/l)	138.2 ± 0.6	139.1 ± 0.4	140.8 ± 0.5*,†
K (mEq/l)	4.02 ± 0.21	3.77 ± 0.09	3.98 ± 0.08
Hb (g/dl)	14.0 ± 0.1	12.5 ± 0.3*	12.8 ± 0.3
HW (g)	1.07 ± 0.04	1.14 ± 0.02	1.20 ± 0.03†
HW/BW (mg/g)	2.42 ± 0.08	2.77 ± 0.04*	2.94 ± 0.09*
KW (g)	1.41 ± 0.07	1.53 ± 0.04	1.66 ± 0.08
KW/BW (mg/g)	3.18 ± 0.12	3.72 ± 0.12	4.07 ± 0.19*

Values are presented as means ± SEM

SNx subtotal nephrectomy (5/6 nephrectomy), *CM* injection of iohexol after administration of indomethacin and L-NAME, *BW* body weight, *SBP* systolic blood pressure, *DBP* diastolic blood pressure, *s-Cre* serum creatinine, *BUN* blood urea nitrogen, *uACR* urine albumin-to-creatinine ratio, *Hb* hemoglobin, *HW* heart weight, *KW* kidney weight

*$p<0.05$ vs Sham, †$p<0.05$ vs SNx.

Signal regulating necroptosis, apoptosis and autophagy in CKD and CIN models

There was no significant difference in protein levels of receptor-interacting serine/threonine-protein kinase (RIP) 1, RIP3, caspase 8, caspase 3 and cleaved-caspase 3 between the Sham and SNx groups. In contrast, all of the proteins that mediate necroptosis and apoptosis were significantly increased in the SNx + CM group (Fig. 2).

As shown in Fig. 3, LC3-II protein level and LC3-II-to-LC3-I ratio were reduced in the SNx + CM group compared with those in the Sham and SNx groups. The level of p62 protein level was lower in the SNx group than in the Sham group, but such a difference was not observed in the SNx + CM group. Together with reduced LC3-II protein level, the finding for p62 suggests that formation of autophagosomes and their processing were suppressed in the SNx + CM group.

Protein levels of AMPK, Akt, S6, Bcl-2 and beclin-1 were comparable in the SNx group and the Sham group, while p70S6K level was lower in the SNx group than in Sham group (Fig. 4). The SNx + CM group showed significantly reduced phosphorylation of Akt and p70S6K compared to that in the SNx and Sham groups. These findings suggest that CM attenuated Akt-mediated pro-survival

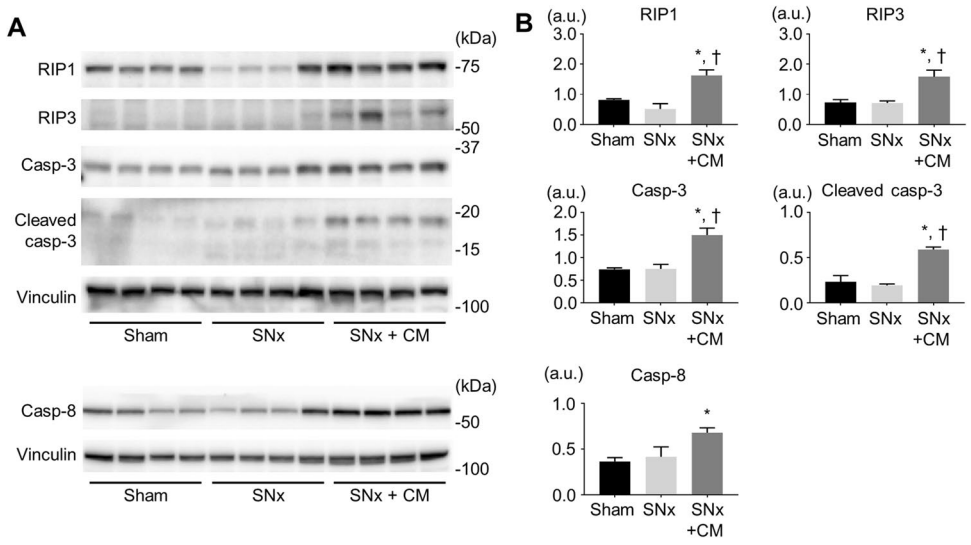

Fig. 2 Levels of RIP proteins and caspases in renal tissues. Representative blots for RIP1, RIP3, caspase 3 (Casp-3) and caspase 8 (Casp-8) (**a**) and quantitative data (**b**). CM induced significant increases in RIP1, RIP3, cleaved Casp-3 and Casp-8, though such changes were not induced by subtotal nephrectomy alone. Each protein level was normalized by vinculin level. $N=4$ in each group. *$p<0.05$ vs Sham, †$p<0.05$ vs SNx. *SNx* subtotal nephrectomy, *CM* administration of iohexol following indomethacin and L-NAME, *kDa* kilodalton, *a.u.* arbitrary unit

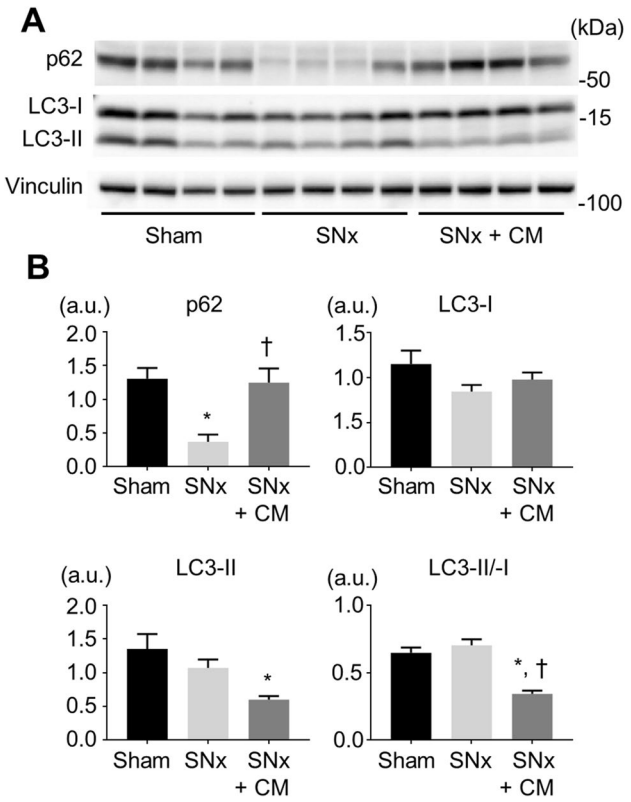

Fig. 3 Levels of p62 and LC3 in renal tissues. Representative blots for p62 and LC3 (**a**) and quantitative data (**b**). Subtotal nephrectomy reduced p62 level without change in LC3 level. CM reduced LC3-II level and increased p62 protein to the level in the sham-operated rats. Each protein level was normalized by vinculin level. $N=4$ in each group. *$p<0.05$ vs Sham, †$p<0.05$ vs SNx. *SNx* subtotal nephrectomy, *CM* administration of iohexol following indomethacin and L-NAME

signals in the kidney, while Akt-mTORC1-mediated suppression of autophagy was also attenuated, possibly counteracting CM-induced suppression of autophagy.

Effects of pharmacological inhibition of necroptosis on CIN

While blood pressure and weights of the heart and kidneys were comparable in the vehicle-treated and Nec-1-treated SNx + CM groups, levels of s-Cre, BUN, log uACR and serum potassium were lower in the Nec-1-treated SNx + CM group (Table 3; Fig. 5a). In addition, ATN score, KIM-1 level and infiltration of CD68-positive macrophages in the kidney were significantly reduced by Nec-1 (Fig. 5b–d). The levels of IL-1β and MCP-1 expression in the kidney were lower in the Nec-1-treated SNx + CM group than in the vehicle-treated SNx + CM group, but the differences did not reach statistical significance (Fig. 5e).

Representative observations for proximal renal tubules by electron microscopy are shown in Fig. 6. In normal SD rats, the ultrastructure of proximal tubules was normal except for tubular collapse and displacement of some nuclei from the basement membrane because of immersion fixation (Fig. 6a, b). In the vehicle-treated SNx + CM group, moderately damaged tubular cells showed loss of microvilli, bleb-like protrusion of the apical cytoplasm (Fig. 6c, d) and increase in vacuoles including autophagic vacuoles (Fig. 6e). In severely damaged cells, swelling and displacement of mitochondria, displacement of the nucleus and disruption of the plasma membrane with extrusion of intracellular organelles were observed (Fig. 6f). The ultrastructural changes in proximal tubular cells caused by CM were attenuated in the Nec-1-treated SNx + CM group (Fig. 6g, h), and there was significant difference in ultrastructural tubular damage score between the vehicle-treated SNx + CM group and the

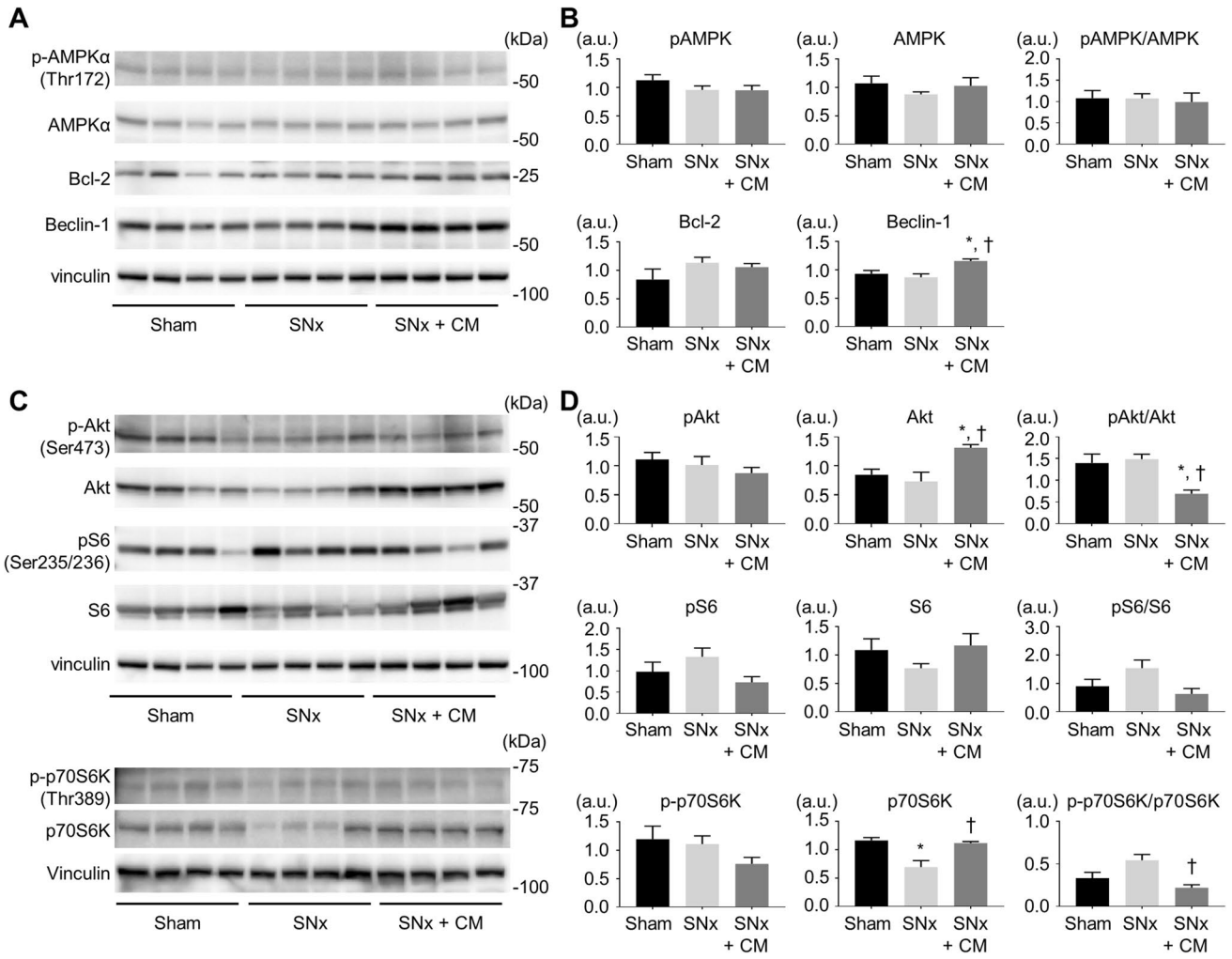

Fig. 4 Signal proteins regulating cell survival and autophagy in renal tissues. Representative immunoblots (**a** and **c**) and quantitative data (**b** and **d**) for phospho-Thr172-AMPKα, total AMPK, Bcl-2, Beclin-1, phospho-Ser473-Akt, total Akt, phospho-Ser235/236-S6, total S6, phospho-Thr389-p70S6K and total p70S6K. Subtotal nephrectomy reduced p70S6K protein level, and CM lowered phosphorylation levels of Akt and p70S6K in rats with subtotal nephrectomy. Each protein level was normalized by vinculin level. The blots of vinculin (**a**) and (**c**, upper) are identical to that in Fig. 3a, because blots of p-AMPK, AMPK, Bcl-2, Beclin-1, p-Akt, Akt, p-S6 and S6 were from the same membrane. The blot of vinculin (**c**, lower) is identical to that in Fig. 2a, because blots of both p-p70S6K and p70S6K were from the same membrane. $N=4$ in each group. $^{*}p<0.05$ vs Sham, $^{\dagger}p<0.05$ vs SNx. *SNx* subtotal nephrectomy, *CM* administration of iohexol following indomethacin and L-NAME, *kDa* kilodalton, *a.u.* arbitrary unit

Nec-1-treated SNx + CM group (Fig. 6i). Each component of ultrastructural tubular damage score is shown in Fig S3.

Discussion

To the best of our knowledge, the present study is the first study providing data suggesting that necroptosis of proximal tubular cells contributes to CIN. In addition, we found that autophagy, which generally functions as protective mechanism was suppressed in CIN, being consistent with our previous findings that pro-necroptotic signaling impairs autophagy, aggravating cell death [11, 12]. How CM activates necroptotic signaling in the kidney remains to be investigated.

Investigations in the past few decades have revealed that hypoperfusion of nephrons and direct toxic effects on renal tubular cells contribute to the development of CIN [2, 4–6, 10]. CM increases plasma and tubular fluid viscosity and also increases vasa recta resistance [10]. CM activates Rho/ROCK signaling [17], NF-κB- [18], and JNK- and p38MAPK-mediated signaling [7] in renal tubular cells. The activation of those signal pathways induces apoptosis of tubular cells and/or upregulates expression of proinflammatory cytokines and receptors [5, 6]. Earlier studies focused on apoptosis as a mechanism of cell death in CIN

Table 3 Blood pressure and renal function data in Protocol 2

	SNx + CM + Ve	SNx + CM + Nec-1	*p* value
N	10	5	
BW (g)	416.9 ± 10.2	421 ± 11.2	0.8076
SBP (mmHg)	130.4 ± 4.0	131.8 ± 5.9	0.8441
DBP (mmHg)	92.6 ± 3.2	100.8 ± 5.4	0.1872
s-Cre (mg/dl)	0.63 ± 0.02	0.56 ± 0.02	0.0120
BUN (mg/dl)	33.9 ± 1.5	28.6 ± 1.2	0.0423
Log uACR (mg/gCre)	5.53 ± 0.23	4.49 ± 0.31	0.0219
Na (mEq/l)	140.9 ± 0.7	139.6 ± 0.2	0.2482
K (mEq/l)	4.04 ± 0.06	3.56 ± 0.08	0.0003
Hb (g/dl)	13.3 ± 0.3	13.0 ± 0.5	0.6153
HW (g)	1.16 ± 0.03	1.12 ± 0.04	0.1460
HW/BW (mg/g)	2.78 ± 0.04	2.66 ± 0.06	0.1687
KW (g)	1.59 ± 0.06	1.55 ± 0.04	0.7541
KW/BW (mg/g)	3.80 ± 0.12	3.64 ± 0.07	0.3676

Values are presented as means ± SEM

SNx: subtotal nephrectomy (5/6 nephrectomy), *CM*: injection of iohexol after administration of indomethacin and L-NAME, *Ve*: vehicle, *Nec-1*: nectostatin-1, *BW*: body weight, *SBP*: systolic blood pressure, *DBP*: diastolic blood pressure, *s-Cre*: serum creatinine, *BUN*: blood urea nitrogen, *uACR*: urine albumin-to-creatinine ratio, *Hb*: hemoglobin, *HW*: heart weight, *KW*: kidney weight

[5, 6], but tubular cells with a necrotic phenotype were also observed in CIN [7]. In the present study, ultrastructural changes of proximal tubular cells after CM injection such as loss of microvilli and displacement of nuclei (Fig. 6) were similar to those after ischemia/reperfusion in earlier studies [19–21], but there were differences such as the shape and size of apical blebs and relatively preserved mitochondrial arrangement. Whether the apparently necrotic cells died mainly by hypoperfusion-induced necrosis or by necroptosis, a novel programmed cell death, cannot be differentiated by morphology.

The present study showed that protein levels of RIP1 and RIP3, proteins participating in necrosome formation, were increased together with levels of caspases 3 and 8 in CIN (Fig. 2). Furthermore, inhibition of RIP1 by Nec-1 suppressed the CM-induced increase in KIM-1 protein and ATN score and attenuated the effects of CM on s-Cre, BUN and uACR (Fig. 5). Together with earlier studies showing the contribution of apoptosis to CIN [7], the present findings indicate that not only apoptosis but also necroptosis of tubular cells contributes to CIN.

Recently, Linkermann et al. proposed that Nec-1 affords protection against CIN by a necroptosis-unrelated mechanism [22]. They used a mouse model of CIN, which was induced by the combination of CM and renal ischemia/reperfusion prior to CM injection. Nec-1 attenuated elevation of s-Cre and BUN 24 h after injection of CM, and this protection was associated with prevention of CM-induced changes in diameters of peri-tubular capillaries. The sensitivity of freshly isolated renal tubular cells to CM-induced LDH release was not changed by knockout of RIP3, suggesting that RIP3-mediated necroptosis was not involved in their mouse model of CIN [22]. In contrast to their results, Nec-1 significantly attenuated the CIN-induced expression of KIM-1 and ATN score (Fig. 5) in our rat CIN model. Thus, the role of necroptosis in CIN is likely to differ in the models used in a study by Linkermann et al. [22] and in the present study, though we cannot exclude the possibility that a part of the protection afforded by Nec-1 in the present study was mediated by a necroptosis-unrelated mechanism.

Accumulating evidence indicates crucial roles of autophagy in protein quality control, energy metabolism and turnover of intracellular organelles [23]. Recent studies have suggested that CMs impair the process of cytoprotective autophagy in renal tubular cells [24, 25]. In a study by Gong et al. [25], the number of autophagic vacuoles and protein levels of LC3-II and beclin-1 were increased by CM in rat kidneys, while p62 level was reduced. In contrast, the protein level of LC3-II was reduced in our model of CIN, while p62 protein level was increased compared with that in CKD controls (Fig. 3). On the other hand, phosphorylation of Akt, p70S6K and S6 was suppressed in the kidney with CIN (Fig. 4c, d), indicating suppression of the Akt-mTORC1 signal pathway. Taken together, the findings suggest that withdrawal of the inhibitory signal via the Akt-mTORC1 pathway was insufficient for overcoming inhibition of autophagy in the present model of CIN. We recently found that the necroptotic RIP1/RIP3 signal pathway inhibits autophagy in cardiomyocytes [11, 12]. Whether similar crosstalk between necroptosis and autophagy is present in renal tubular cells remains to be investigated.

An autoamplification loop between cell necrosis and inflammation has been proposed and is called necroinflammation [26]. Necroptosis results in release of danger-associated molecular patterns (DAMPs), which recruit macrophages and increase production of proinflammatory cytokines and chemokines. The proinflammatory responses lead to activation of receptors that trigger necroptotic signaling, amplifying necroinflammation and tissue injury. In the present study, Nec-1 significantly reduced infiltration of macrophages, while its suppressive effects on IL-1β and MCP-1 were not statistically significant. The findings suggest that the protective effect of Nec-1 was primarily mediated by suppression of necroptosis of tubular cells, though the possibility of its secondary effects on proinflammatory cytokines cannot be excluded.

There are limitations in the present study. First, since we administered Nec-1 both before and after injection of CM, it is not clear whether Nec-1 prevented and/or attenuated CIN in the present model of CIN. Second, we used whole kidney

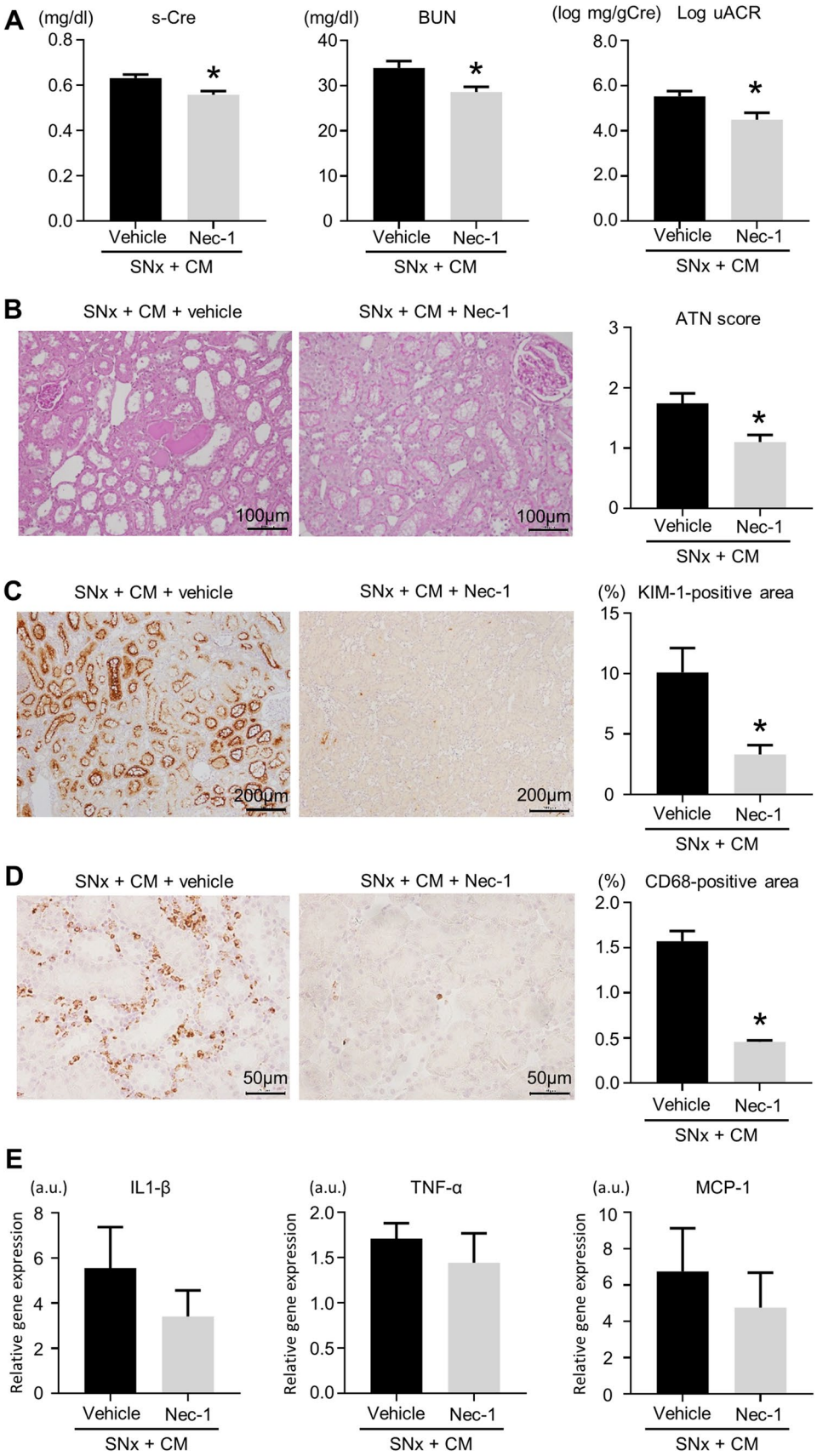

Fig. 5 Effects of necrostatin-1 on contrast-induced nephropathy. Serum and urinary indices of renal dysfunction (**a**) and histological indices of renal tissue damage, ATN score (**b**) and KIM-1-positive area (**c**), were significantly improved by necrostatin-1 injection. The infiltration of CD68-positive macrophages shown in the SNx + CM group was significantly reduced in the Nec-1-treated SNx + CM group (**d**). The expression levels of IL-1β, TNF-α and MCP-1 in the kidney tended to be reduced by Nec-1, though the differences were not statistically significant (**e**). $N = 10$ in SNx + CN + Vehicle and $N = 5$ in SNx + CM + Nec-1 in **a**, N = 6 in each group in **b**–**e**. *$p < 0.05$ vs SNx + CM + vehicle. *s-Cre* serum creatinine, *Nec-1* necrostatin-1, *SNx* subtotal nephrectomy, *CM* administration of iohexol following indomethacin and L-NAME, *BUN* blood urea nitrogen, *ATN* acute tubular necrosis

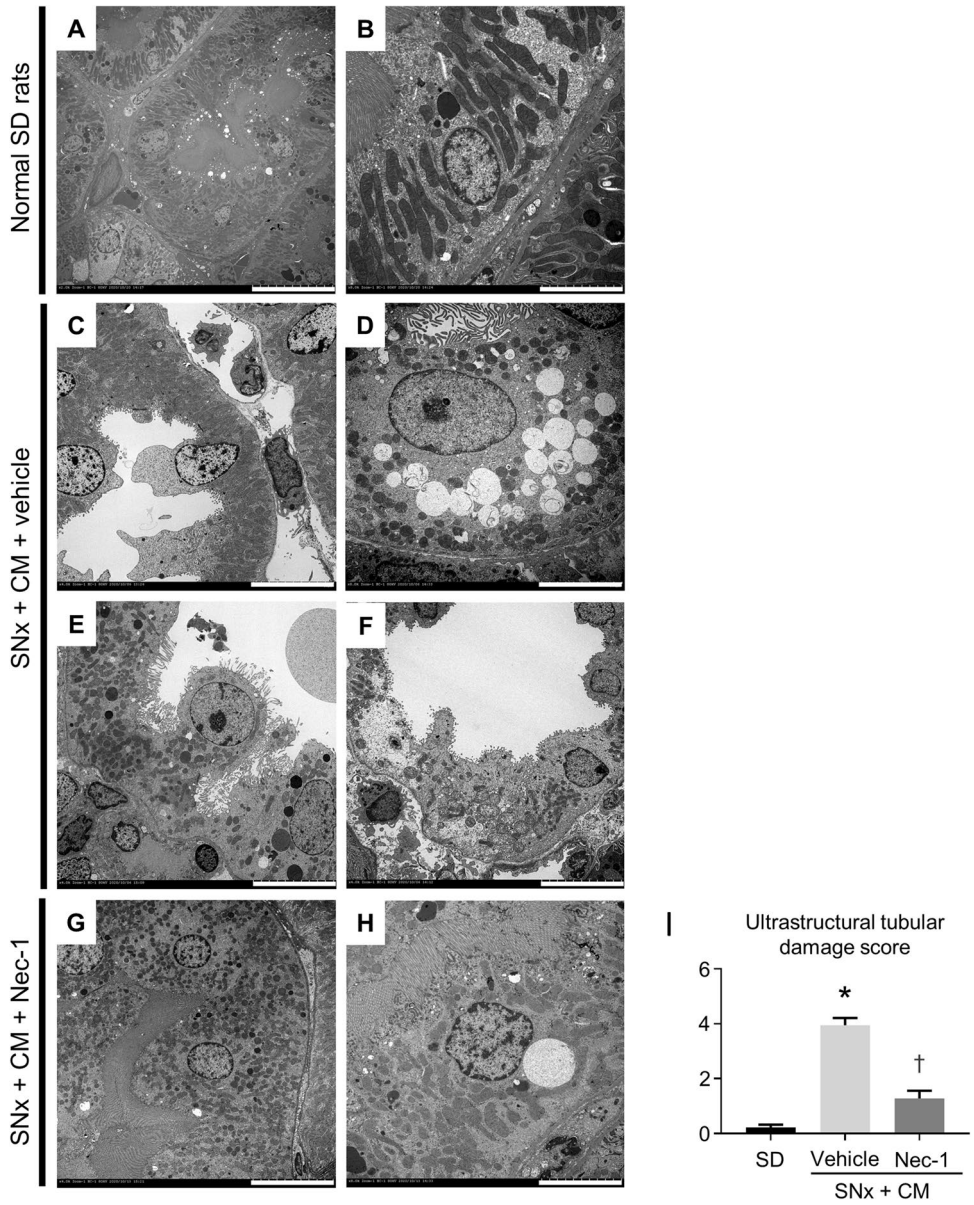

Fig. 6 Electron micrographs of proximal tubular cells. **a** and **b** Normal Sprague–Dawley (SD) rats. Original magnification ×2,000 in **a** and ×8,000 in **b**. Scale bars are 20 μm in **a** and 5.0 μm in **b**. Because of immersion fixation, there are tubular collapse and displacement of some nuclei from the basement membrane were observed. **c**–**f** Vehicle-treated SNx + CM group. In the modestly damaged area (**c**), mitochondrial morphology and arrangement were relatively preserved, though blebbing of the apical cytoplasm and displacement of mitochondria were observed. In the more severely damaged area, disarranged mitochondria (**d**, **e**, **f**), increased vacuoles (**d**), marked displacement of the nucleus (**e**) and swelling of mitochondria and flattening of the cell (**f**) were observed. Original magnification ×4,000 in **c**, **e**, and **f**, ×8,000 in **d**. Scale bars are 10 μm in **c**, **e**, and **f** and 5.0 μm in **d**. **g**, **h**: Nec-1-treated SNx + CM group. Nuclei and mitochondria were displaced towards the cell apex, but microvilli and height of cells were preserved. Original magnification ×4,000 in **g** and ×8,000 in **h**. Scale bars are 10 μm in **g** and 5.0 μm in **h**. **i** Ultrastructural tubular damage scores per cell cross section of proximal tubule in normal controls (SD), vehicle-treated SNx + CM group and Nec-1-treated SNx + CM group. $^{*}p < 0.05$ vs SD, $^{\dagger}p < 0.05$ vs SNx + CM + vehicle. *SD* Sprague–Dawley, *Nec-1* necrostatin-1, *SNx* subtotal nephrectomy, *CM* administration of iohexol following indomethacin and L-NAME

tissues for Western blotting and RT-PCR, and a significant change in a protein or mRNA in proximal tubules might have been masked by changes in other types of cells. Third, we determined renal function and renal pathology only at 48 h after CM injection, and thus the protective effects of Nec-1 on the time course of renal function recovery after development of CIN remain unclear.

In conclusion, a significant contribution of necroptosis to CIN in a rat model of CKD was supported by the findings that CIN was accompanied by up-regulation of RIP1 and

RIP3 expression and by reduced LC3-II protein with accumulation of p62, possibly reflecting impaired autophagy by necroptotic signaling, in the renal tissue and that RIP1 inhibition by Nec-1 significantly attenuated the severity of CIN assessed by s-Cre, BUN, tissue ATN score, tissue expression of KIM-1 and electron microscopy.

Supplementary Information The online version contains supplementary material available at https://doi.org/10.1007/s10157-021-02048-1.

Funding This study was supported by a Grant for Education and Research from Sapporo Medical University 2019 and partly by a Grant from Otsuka Pharmaceutical Co., Tokyo, Japan.

Declarations

Conflict of interest This study was supported partly by a grant from Otsuka Pharmaceutical Co., Tokyo, Japan.

Human and animal rights This article does not contain any studies with human. All animal experiments were performed in Animal Research Center, Sapporo Medical University in strict accordance with the Guide for the Care and Use of Laboratory Animals published by the United States National Institutes of Health.

Ethical approval This study was approved by the Animal Use Committee of Sapporo Medical University (#16–088).

References

1. James MT, Samuel SM, Manning MA, Tonelli M, Ghali WA, Faris P, et al. Contrast-induced acute kidney injury and risk of adverse clinical outcomes after coronary angiography: a systematic review and meta-analysis. Circ Cardiovasc Interv. 2013;6:37–43.
2. Azzalini L, Spagnoli V, Ly HQ. Contrast-induced nephropathy: from pathophysiology to preventive strategies. Can J Cardiol. 2016;32:247–55.
3. Mehran R, Aymong ED, Nikolsky E, Lasic Z, Iakovou I, Fahy M, et al. A simple risk score for prediction of contrast-induced nephropathy after percutaneous coronary intervention: Development and initial validation. J Am Col Cardiol. 2004;44:1393–9.
4. Heyman SN, Rosen S, Rosenberger C. Renal parenchymal hypoxia, hypoxia adaptation, and the pathogenesis of radiocontrast nephropathy. Clin J Am Soc Nephrol. 2008;3:288–96.
5. Mehran R, Dangas GD, Weisbord SD. Contrast-associated acute kidney injury. N Engl J Med. 2019;380:2146–55.
6. Tumlin J, Stacul F, Adam A, Becker CR, Davidson C, Lameire N, et al. Pathophysiology of contrast-induced nephropathy. Am J Cardiol. 2006;98:14K-20K.
7. Quintavalle C, Brenca M, de Micco F, Fiore D, Romano S, Romano MF, et al. In vivo and in vitro assessment of pathways involved in contrast media-induced renal cells apoptosis. Cell Death Dis. 2011;2:e155.
8. Linkermann A, Bräsen JH, Darding M, Jin MK, Sanz AB, Heller JO, et al. Two independent pathways of regulated necrosis mediate ischemia-reperfusion injury. Proc Natl Acad Sci USA. 2013;110:12024–9.
9. Zhu Y, Cui H, Xia Y, Gan H. RIPK3-mediated necroptosis and apoptosis contributes to renal tubular cell progressive loss and chronic kidney disease progression in rats. PLoS ONE. 2016;11:e0156729.
10. Seeliger E, Sendeski M, Rihal CS, Persson PB. Contrast-induced kidney injury: mechanisms, risk factors, and prevention. Eur Heart J. 2012;33:2007–15.
11. Ogasawara M, Yano T, Tanno M, Abe K, Ishikawa S, Miki T, et al. Suppression of autophagic flux contributes to cardiomyocyte death by activation of necroptotic pathways. J Mol Cell Cardiol. 2017;108:203–13.
12. Abe K, Yano T, Tanno M, Miki T, Kuno A, Sato T, et al. mTORC1 inhibition attenuates necroptosis through RIP1 inhibition-mediated TFEB activation. Biochim Biophys Acta Mol Basis Dis. 2019;1865:165552.
13. Nishizawa K, Yano T, Tanno M, Miki T, Kuno A, Tobisawa T, et al. Chronic treatment with an erythropoietin receptor ligand prevents chronic kidney disease-induced enlargement of myocardial infarct size. Hypertension. 2016;68:697–706.
14. Agmon Y, Peleg H, Greenfeld Z, Rosen S, Brezis M. Nitric oxide and prostanoids protect the renal outer medulla from radiocontrast toxicity in the rat. J Clin Invest. 1994;94:1069–75.
15. Muratsubaki S, Kuno A, Tanno M, Miki T, Yano T, Sugawara H, et al. Suppressed autophagic response underlies augmentation of renal ischemia/reperfusion injury by type 2 diabetes. Sci Rep. 2017;7:5311.
16. Kimura Y, Kuno A, Tanno M, Sato T, Ohno K, Shibata S, et al. Canagliflozin, a sodium–glucose cotransporter 2 inhibitor, normalizes renal susceptibility to type 1 cardiorenal syndrome through reduction of renal oxidative stress in diabetic rats. J Diabetes Investig. 2019;10:933–46.
17. Wang Y, Zhang H, Yang Z, Miao D, Zhang D. Rho kinase inhibitor, fasudil, attenuates contrast-induced acute kidney injury. Basic Clin Pharmacol Toxicol. 2018;122:278–87.
18. MacHado RA, Constantino LDS, Tomasi CD, Rojas HA, Vuolo FS, Vitto MF, et al. Sodium butyrate decreases the activation of NF-κB reducing inflammation and oxidative damage in the kidney of rats subjected to contrast-induced nephropathy. Nephrol Dial Transplant. 2012;27:3136–40.
19. Reimer KA, Ganote CE, Jennings RB. Alterations in renal cortex following ischemic injury. 3. Ultrastructure of proximal tubules after ischemia or autolysis. Lab Invest. 1972;26:347–63.
20. Glaumann B, Glaumann H, Berezesky IK, Trump BF. Studies on the pathogenesis of ischemic cell injury II Morphological changes of the pars convoluta (P1 and P2) of the proximal tubule of the rat kidney made ischemic in vivo. Virchows Arch B Cell Pathol. 1975;19:281–302.
21. Glaumann B, Glaumann H, Trump BF. Studies of cellular recovery from injury. III. Ultrastructural studies on the recovery of the pars recta of the proximal tubule (P3 segment) of the rat kidney from temporary ischemia. Virchows Arch B Cell Pathol. 1977;25:281–308.
22. Linkermann A, Heller JO, Prókai Á, Weinberg JM, de Zen F, Himmerkus N, et al. The RIP1-kinase inhibitor Necrostatin-1 prevents osmotic nephrosis and contrast-induced AKI in mice. J Am Soc Nephrol. 2013;24:1545–57.
23. Dikic I, Elazar Z. Mechanism and medical implications of mammalian autophagy. Nat Rev Mol Cell Biol. 2018;19:349–64.
24. Lei R, Zhao F, Tang CY, Luo M, Yang SK, Cheng W, et al. Mitophagy plays a protective role in iodinated contrast-induced acute renal tubular epithelial cells injury. Cell Physiol Biochem. 2018;46:975–85.
25. Gong X, Duan Y, Zheng J, Ye Z, Hei TK. Tetramethylpyrazine prevents contrast-induced nephropathy via modulating tubular cell mitophagy and suppressing mitochondrial fragmentation, CCL2/CCR2-mediated inflammation, and intestinal injury. Oxid Med Cell Longev. 2019;2019:7096912.
26. Mulay SR, Linkermann A, Anders HJ. Necroinflammation in kidney disease. J Am Soc Nephrol. 2016;27:27–39.

Supplementary file1

Involvement of necroptosis in contrast-induced nephropathy in a rat CKD model

Satoru Shibata, Norihito Moniwa, Atsushi Kuno, Ayumu Kimura, Wataru Ohwada, Hirohito Sugawara, Yufu Gocho, Marenao Tanaka, Toshiyuki Yano, Masato Furuhashi, Masaya Tanno, Takayuki Miki and Tetsuji Miura

Department of Cardiovascular, Renal and Metabolic Medicine, Sapporo Medical University School of Medicine, Sapporo, Japan

Materials and Methods

Western blotting

Western blotting was performed as previously reported (1) using primary antibodies listed in Table 1. Briefly, frozen kidney tissue samples were homogenized in ice-cold buffer (CelLyticTM MT Cell Lysis Reagent, Sigma-Aldrich, St. Louis, MO) including 0.5 mmol/l Na3VO4, a protease inhibitor cocktail (Complete mini, Roche Molecular Biochemicals, Mannheim, Germany) and 1 mmol/l phenylmethylsulfonyl fluoride. The supernatant of the homogenate was obtained after centrifugation at 15,000 g for 15 min at 4°C. Equal amounts of proteins were electrophoresed on polyacrylamide gels and then blotted onto PVDF membranes (Millipore, Bedford, MA). After blocking with a TBS-T buffer containing 5% nonfat dry milk or 5% BSA, the blots were incubated with antibodies listed in Table 1. Immunoblotted proteins were visualized by using an Immobilon Western Detection Kit (Millipore, Billerica, MA). Densitometry of blotted proteins was performed by using Fusion Solo 7S with Fusion-Capt software (Vilber Lourmat, Marne-la-Vallee, France).

Real-time PCR

mRNA levels of KIM-1, IL-1β, TNF-α and MCP-1 in kidneys were determined by real-time PCR as described previously (2). Briefly, messenger RNA was isolated from frozen tissues by using an RNeasy Fibrous Tissue Mini Kit (Qiagen, Valencia, CA, USA). A SuperScript VILOTM cDNA Synthesis Kit (Life Technologies, Thermo Fisher Scientific, Waltham, MA, USA) was used to synthesize complementary DNA. DNA amplification was carried out in ABI PRISM7500 (Life Technologies) by using Taqman Universal PCR Master Mix.

References

1. Muratsubaki S, Kuno A, Tanno M, Miki T, Yano T, Sugawara H, et al. Suppressed autophagic response underlies augmentation of renal ischemia/reperfusion injury by type 2 diabetes. Sci Rep. 2017;7:5311.
2. Kimura Y, Kuno A, Tanno M, Sato T, Ohno K, Shibata S, et al. Canagliflozin, a sodium–glucose cotransporter 2 inhibitor, normalizes renal susceptibility to type 1 cardiorenal syndrome through reduction of renal oxidative stress in diabetic rats. J Diabetes Investig. 2019;10:933–946.

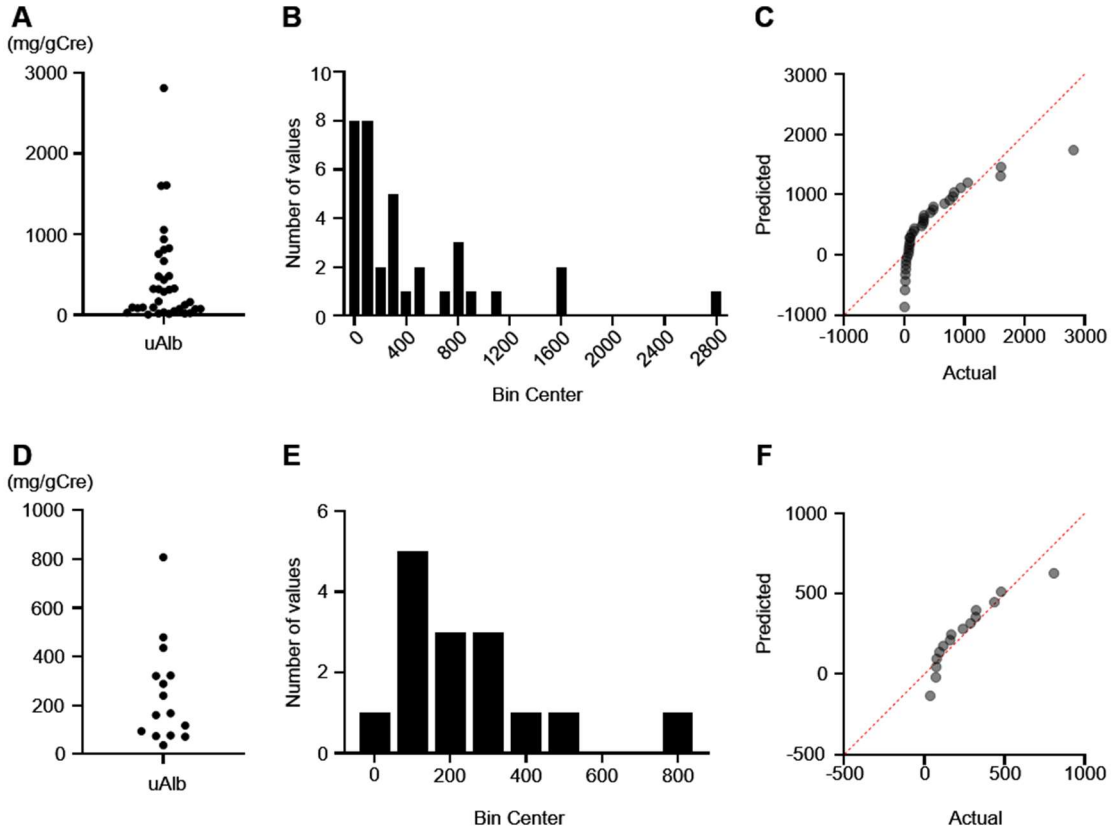

Fig. S1. Distribution of urinary albumin-to-creatinine ratio data.

Urinary albumin-to-creatinine ratio (uACR) of all rats (A), histogram of uACR (B), and quantile-quantile (Q-Q) plot of uACR (C) in Protocol 1. uACR of all rats (D), histogram of uACR (E), and Q-Q plot of uACR (F) in Protocol 2. uACR in both protocols showed a non-normal distribution by the Shapiro-Wilk test ($p<0.05$ in both protocols).

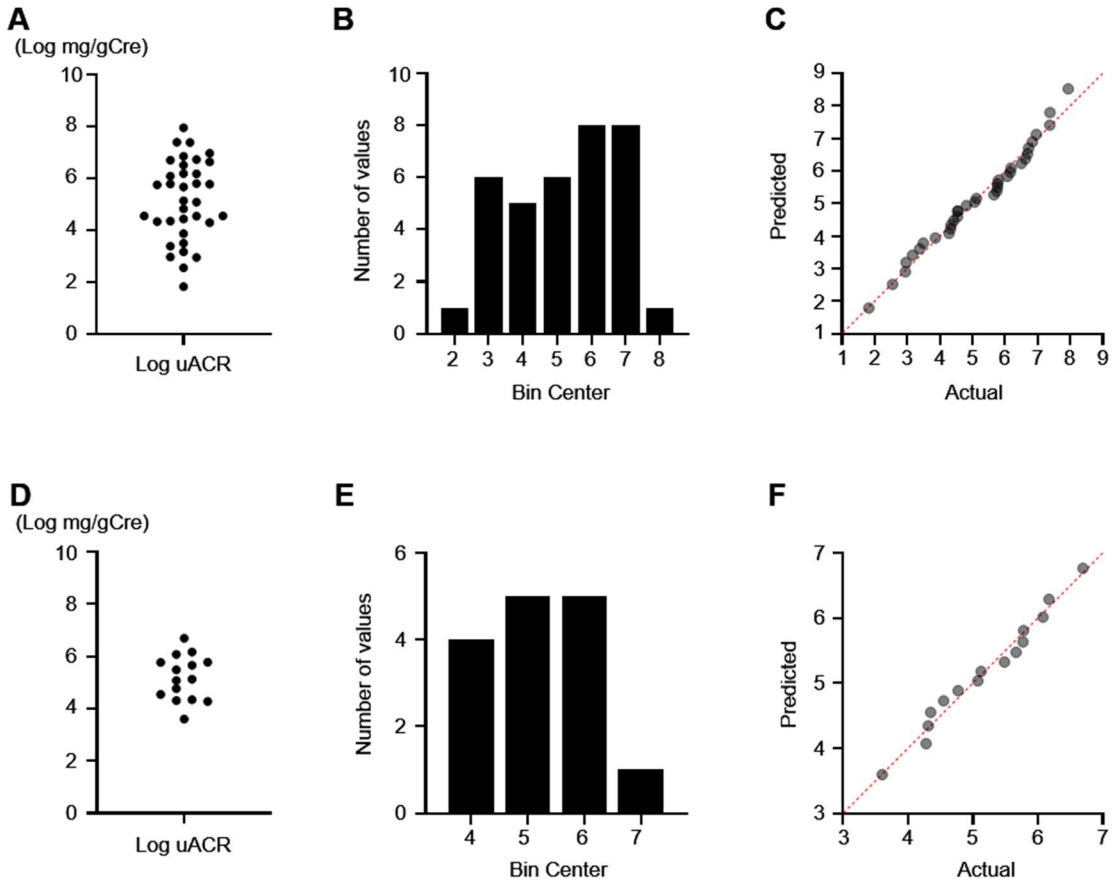

Fig. S2. Distribution of logarithmically transformed data for urinary albumin-to-creatinine ratio.

Log urinary albumin-to-creatinine ratio (uACR) of all rats (A), histogram of log uACR (B), and quantile-quantile (Q-Q) plot of log uACR (C) in Protocol 1. Log uACR of all rats (D), histogram of log uACR (E), and Q-Q plot of log uACR (F) in Protocol 2. A normal distribution of the data was confirmed by the Shapiro-Wilk test (p=0.59 in Protocol 1 and p=0.91 in Protocol 2).

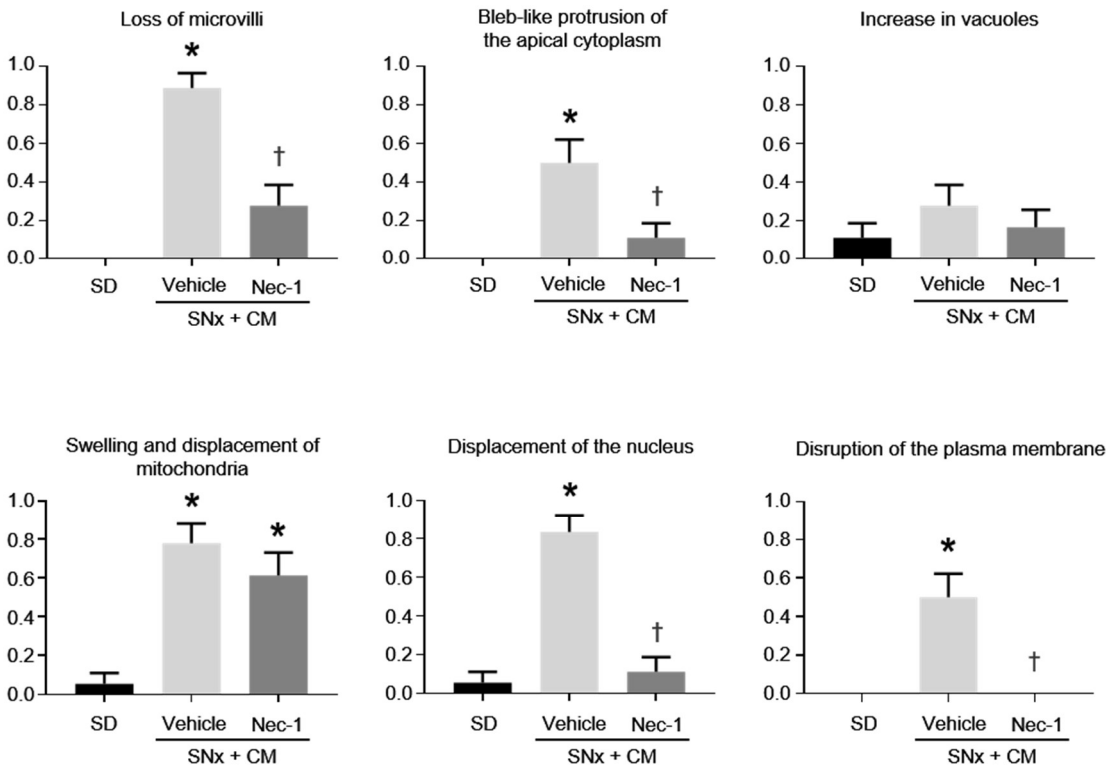

Fig. S3. Components of ultrastructural tubular damage scores in Protocol 2.
Loss of microvilli (A), bleb-like protrusion of the apical cytoplasm (B), increase in vacuoles (C), swelling and/or displacement of mitochondria (D), displacement of the nucleus (E), and disruption of the plasma membrane (F) per cross-section of proximal tubule in normal controls (SD), vehicle-treated SNx+CM group and Nec-1-treated SNx+CM group are shown. *: $p<0.05$ vs SD, †: $p<0.05$ vs SNx+CM+vehicle. SD: Sprague-Dawley, Nec-1: necrostatin-1, SNx: subtotal nephrectomy, CM: administration of iohexol following indomethacin and L-NAME.